

بِسْمِ اللَّهِ الرَّحْمَنِ الرَّحِيمِ

۱۱۰۵۱۸

۱۷/۱/۱۰۷۷۹۹
۱۸۷/۱۱۰



Razi University

Faculty of science
Department of physics

PhD. Thesis

**Investigation of magnetic and nonmagnetic impurity effects
on the electronic Properties of carbon nanotubes**

Supervisor:

Dr. Rostam Moradian

By:

Ali Fathalian

July 2008

۱۱۸۱۰

۸۷/۱۱/۱۰۷۷۶۴
۸۸/۱/۱۵



دانشگاه رازی
دانشکده علوم
گروه فیزیک

پایان نامه جهت اخذ درجه دکتری رشته ی فیزیک
گرایش ماده چگال

عنوان پایان نامه

بررسی اثر ناخالصی های مغناطیسی و غیر مغناطیسی بر روی
خواص الکترونی نانولوله های کربنی

کتابخانه دانشگاه رازی
تاسیس ۱۳۸۸

استاد راهنما:

دکتر رستم مرادیان

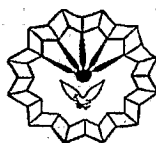
نگارش:

علی فتحعلیان

تیرماه ۱۳۸۷

۱۳۸۸ / ۱ / ۲۱

۱۱۰۵۱۵



Razi University

Faculty of Science
Department of Physics

PhD Thesis

Investigation of magnetic and nonmagnetic impurity effects on the electronic properties of carbon nanotube

By:

Ali Fathalian

Evaluated and approved by thesis committee: as.. *Excellent*

Dr. R. Moradian	Supervisor	<i>R. Moradian</i>	Associ.Prof
Dr.A.R.Saffarzadeh	External Examiner.....	<i>Saf</i>	Associ.Prof
Dr.A.H.Alizadeh	Internal Examiner.....	<i>A. Alizadeh</i>	Assistant.Prof
Dr.S.M.Elahi	Internal Examiner.....	<i>S.M. Elahi</i>	Associ.Prof

July 2008

Acknowledgment

I would like express my since appreciate and thankfulness to my supervisor Prof. Rostam Moradian for his continuous academic guidance and support during my PhD study. I would also like to express my gratitude to Prof. Mohammad Elahi and Dr. Samad Behroozi for their encouragements. This work won't be completed without the help of my friends: Dr. Shahpoor Moradi, Dr. Hamze Mousavi, Dr. Daryoush Souri, Nader Ghobadi, Reza Kakavandi and Yavar Mohammadi. Finally I wish to thank my parents, my brother and my sisters for their patience and support.

Abstract

In chapter-2 the possibility of a ferromagnetic semiconductor single-wall carbon nanotube, where ferromagnetism is due to coupling between a doped magnetic impurity on a zigzag SWCNT and electron spin, is investigated. By increasing impurity concentrations the semiconducting gap of spin up electrons in the density of states is closed, hence a semiconductor to semi-metallic disordered graphene phase transition takes place. In chapter-3 effects of magnetic impurity doping on the Curie critical temperature (T_c) of semiconducting carbon nanotubes is investigated. Variation of T_c as a function of impurity concentration for different coupling constant (J), and spin value (S) are calculated. By increasing J and S , the critical temperature is increased. In chapter-4 superconductivity in the single-walled carbon nanotubes, is investigated. The results illustrate that metallic zigzag single-walled carbon nanotubes have higher T_c than armchair SWCNT with approximately same diameters and T_c decreases by increasing diameter. In chapter-5 effects of inter wall hopping on the electronic properties of double-wall carbon nanotubes using tight-binding model, is investigated. The results illustrate by switching inter-wall interactions a valley opened in the $(n, n)@(2n, 2n)$ walls local density of states, although both walls remained metallic. For the case of $(n, 0)@(2n, 0)$ where n is not multiple of 3 a semiconducting to metallic phase transition is found, while when n is multiple of 3 both inner and outer walls remained metallic.

Contents

1	<i>Introduction on carbon nanotubes</i>	1
1.1	<i>Introduction</i>	2
1.2	<i>Allotropes of carbon</i>	3
1.2.1	<i>Diamond</i>	3
1.2.2	<i>Graphite</i>	4
1.2.3	<i>Buckminsterfullerenes</i>	5
1.2.4	<i>Carbon nanotubes</i>	6
1.2.5	<i>Highly oriented pyrolytic graphite</i>	16
1.2.6	<i>Glassy carbon</i>	17
1.2.7	<i>Carbon Fibres</i>	17
1.2.8	<i>Amorphous carbon</i>	18
1.3	<i>Synthesis of carbon nanotubes</i>	18
1.3.1	<i>Arc-discharge technique</i>	18
1.3.2	<i>Laser ablation</i>	19
1.3.3	<i>CVD-method</i>	20
1.4	<i>Growth mechanism of carbon nanotubes</i>	25
1.5	<i>Electronic properties of nanotubes</i>	28
1.6	<i>Applications of carbon nanotubes</i>	31
1.6.1	<i>Cathode-Ray Lighting Elements</i>	31

1.6.2	<i>Flat Panel Display</i>	31
1.6.3	<i>Nanoprobes and Sensors</i>	34
1.6.4	<i>Templates</i>	37
2	<i>Ferromagnetic semiconductor single-wall carbon nanotubes</i>	43
2.1	<i>Introduction</i>	44
2.2	<i>Hubbard model</i>	45
2.2.1	<i>Tight binding picture of solids</i>	48
2.3	<i>Model and formalism</i>	50
2.4	<i>Coherent potential approximation(CPA)</i>	56
2.5	<i>Results and discussion</i>	58
2.6	<i>Conclusion</i>	68
3	<i>Magnetic impurity effects in zigzag carbon nanotubes</i>	69
3.1	<i>Introduction</i>	70
3.2	<i>Model and formalism</i>	70
3.3	<i>Results and discussion</i>	72
3.4	<i>Conclusion</i>	73
4	<i>Investigation of superconductivity in the single wall carbon nan-</i>	
	<i>otubes</i>	77
4.1	<i>Introduction</i>	78
4.2	<i>Model and Bogoliubov de Gennes equation</i>	79
4.2.1	<i>Bogoliubov de Genne equation for singlet superconductors</i>	90
4.3	<i>General solution of the Bogoliubov de Gennes equation</i>	91
4.4	<i>Coherent Potential approximation (CPA)</i>	93
4.5	<i>Local order parameter</i>	96

4.6	<i>Calculation of T_c in the CPA formalism, results and discussion</i>	97
4.7	<i>Results and discussion</i>	99
4.8	<i>Conclusion</i>	102
5	<i>Effects of inter wall hopping on the electronic properties of double-wall carbon nanotubes</i>	105
5.1	<i>Introduction</i>	106
5.2	<i>Model and formalism</i>	106
5.3	<i>Results and discussion</i>	113
5.4	<i>Conclusion</i>	118
	Bibliographie	120

Chapter 1

Introduction on carbon nanotubes

1.1 *Introduction*

Carbon is the most versatile element in the periodic table, owing to the type, strength, and number of bonds it can form with many different elements. The diversity of bonds and their corresponding geometries enable the existence of structural isomers, geometric isomers, and enantiomers. These are found in large, complex, and diverse structures and allow for an endless variety of organic molecules. The properties of carbon are a direct consequence of the arrangement of electrons around the nucleus of the atom. There are six electrons in a carbon atom, shared evenly between the $1s$, $2s$, and $2p$ orbitals. Since the $2p$ atomic orbitals can hold up to six electrons, carbon can make up to four bonds; however, the valence electrons, involved in chemical bonding, occupy both the $2s$ and $2p$ orbitals. Covalent bonds are formed by promotion of the $2s$ electrons to one or more $2p$ orbitals; the resulting hybridized orbitals are the sum of the original orbitals. Depending on how many p orbitals are involved, this can happen in three different ways. In the first type of hybridization, the $2s$ orbital pairs with one of the $2p$ orbitals, forming two hybridized sp^1 (figure1.1a) orbitals in a linear geometry, separated by an angle of 180° . The second type of hybridization involves the $2s$ orbital hybridizing with two $2p$ orbitals; as a result, three sp^2 (figure1.1b) orbitals are formed. These are on the same plane separated by an angle of 120° . In the third hybridization, one $2s$ orbital hybridizes with the three $2p$ orbitals, yielding four sp^3 orbitals separated by an angle of 109.5° . sp^3 (figure1.1c) hybridization yields the characteristic tetrahedral arrangements of the bonds. In all three cases, the energy required to hybridize the

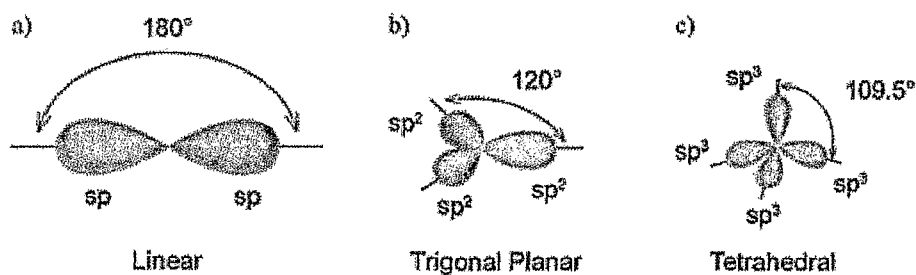


Figure 1.1: The different hybridisations of carbon a) sp^1 , b) sp^2 , c) sp^3

atomic orbitals is given by the free energy of forming chemical bonds with other atoms. Carbon can bind in a sigma (σ) bond and a pi (π) bond while forming a molecule; the final molecular structure depends on the level of hybridization of the carbon orbitals. An sp^1 hybridized carbon atom can make two σ bonds and two π bonds, sp^2 hybridized carbon forms three σ bonds and one π bond, and an sp^3 hybridized carbon atom forms four π bonds. The number and nature of the bonds determine the geometry and properties of carbon allotropes.

1.2 Allotropes of carbon

Carbon in the solid phase can exist in three allotropic forms: graphite, diamond, and buckminsterfullerene (Fig.1.1).

1.2.1 Diamond

Diamond has a crystalline structure where each sp^3 hybridized carbon atom is bonded to four others in a tetrahedral arrangement. The crystalline network gives diamond its hardness (it is the hardest substance known) and excellent heat conduction

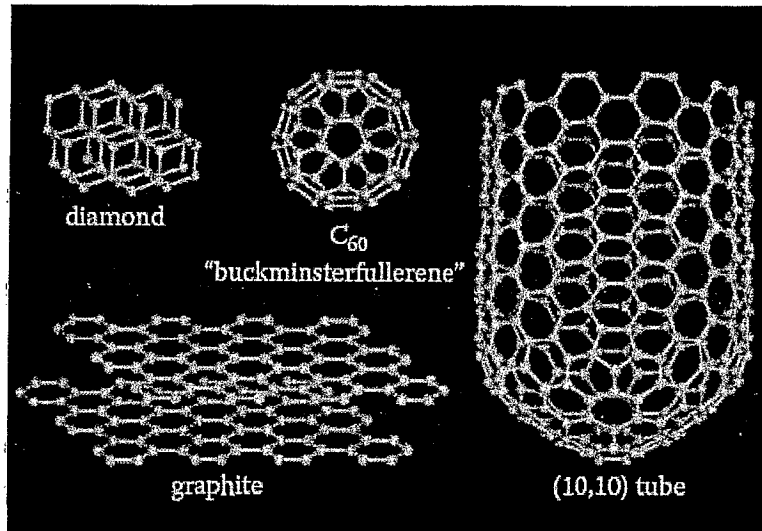


Figure 1.2: The three allotropes of carbon.

properties (about five times better than copper). The sp^3 hybridized bonds account for its electrically insulating property and optical transparency.

1.2.2 Graphite

Graphite is made by layered planar sheets of sp^2 hybridized carbon atoms bonded together in a hexagonal network. The different geometry of the chemical bonds makes graphite soft, slippery, opaque, and electrically conductive. In contrast to diamond, each carbon atom in a graphite sheet is bonded to only three other atoms; electrons can move freely from an unhybridized p orbital to another, forming an endless delocalized π bond network that gives rise to the electrical conductivity. In the most common hexagonal crystal form of graphite the layers are stacked in an *ABAB...* sequence (called Bernal stacking) (Fig.1.3). The in-plane nearest neighbour distance a_{C-C} is 1.421\AA [1] and the lattice constant is $a_0 = 2.461\text{\AA}$. The c-axis lattice constant is $c_0 = 6.708\text{\AA}$ and the interplanar distance $c_0/2$.

A minor component of well-crystallised graphite is the rhombohedral form of graphite

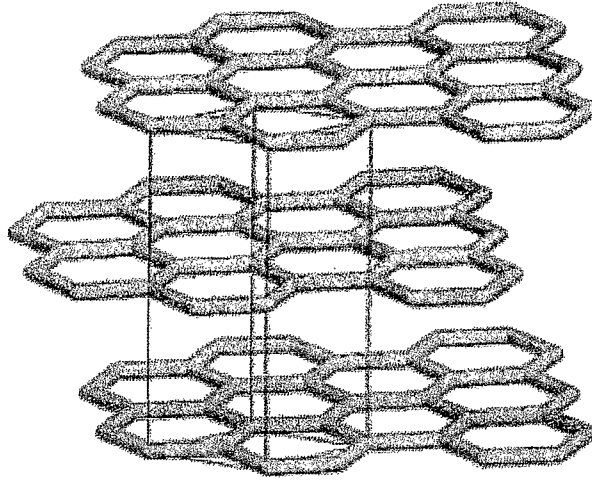


Figure 1.3: hexagonal graphite (*ABAB* stacking) with unit cell

in which the graphene (single layer of crystalline graphite) layers are stacked in the *ABCABC...* sequence. The lattice constant is also $a_0 = 2.456\text{\AA}$ and $c_0 = 3.(3.438) = 10.044\text{\AA}$. The Bernal *AB* stacking of graphite is more stable than the *ABC* stacking. The density of both forms of graphite is 2.26g.cm^{-3} [2]. The weak interlayer bonding of graphite originates from the small overlap of the p_z -orbitals between atoms of adjacent layers and not to Van der Waals bonding.

1.2.3 *Buckminsterfullerenes*

Buckminsterfullerenes, or fullerenes, are the third allotrope of carbon and consist of a family of spheroidal or cylindrical molecules with all the carbon atoms sp^2 hybridized. Experimental and theoretical work has shown that the most stable form of carbon clusters form linear chains [3] for clusters of up to about 10 atoms. For clusters that have 10 to 30 carbon atoms the ring is the most stable form [4]. Carbon clusters between 30 and 40 carbon atoms are unlikely and clusters above 40 atoms form cage structures. Especially stable structures are the C_{60} , whose structure was identified the first time by

Kroto et al. in 1985 [5]. The carbon atoms are located at the 60 vertices of a truncated icosahedron that has 90 edges and 32 faces of which 12 are pentagons and 20 hexagons, consistent with Eulers theorem for polyhedra:

$$f + v = e + 2 \quad (1.1)$$

where f , v and e are the number of faces, vertices, and edges of the polyhedra. The average nearest-neighbour CC distance is with $a_{C-C} = 1.44\text{\AA}$ almost equal to that in graphite. Each carbon atom is trigonally bonded to three other carbon atoms in an sp^2 -derived bonding configuration. The curvature of the trigonal bonds in C_{60} leads to some admixture of sp^3 bonding, characteristic for tetrahedrally bonded diamond, but absent in graphite [6]. Further stable fullerenes are C_{70} , C_{78} , C_{80}

1.2.4 Carbon nanotubes

a) History

Fullerenes were discovered in 1985 by Rick Smalley and coworkers[7]. C_{60} was the first fullerene to be discovered. C_{60} , or bucky ball, is a soccer ball (icosahedral)-shaped molecule with 60 carbon atoms bonded together in pentagons and hexagons. The carbon atoms are sp^2 hybridized, but in contrast to graphite, they are not arranged on a plane. The geometry of C_{60} strains the bonds of the sp^2 hybridized carbon atoms, creating new properties for C_{60} . Graphite is a semimetal, whereas C_{60} is a semiconductor.

The discovery of C_{60} was, like many other scientific breakthroughs, an accident. It started because Kroto was interested in interstellar dust, the long-chain polyynes formed by red giant stars. Smalley and Curl developed a technique to analyze atom clusters produced by laser vaporization with time-of-flight mass spectrometry, which caught Kroto's attention. When they used a graphite target, they could produce and analyze the long chain polyynes (Fig.1.4a). In September of 1985, the collaborators experimented

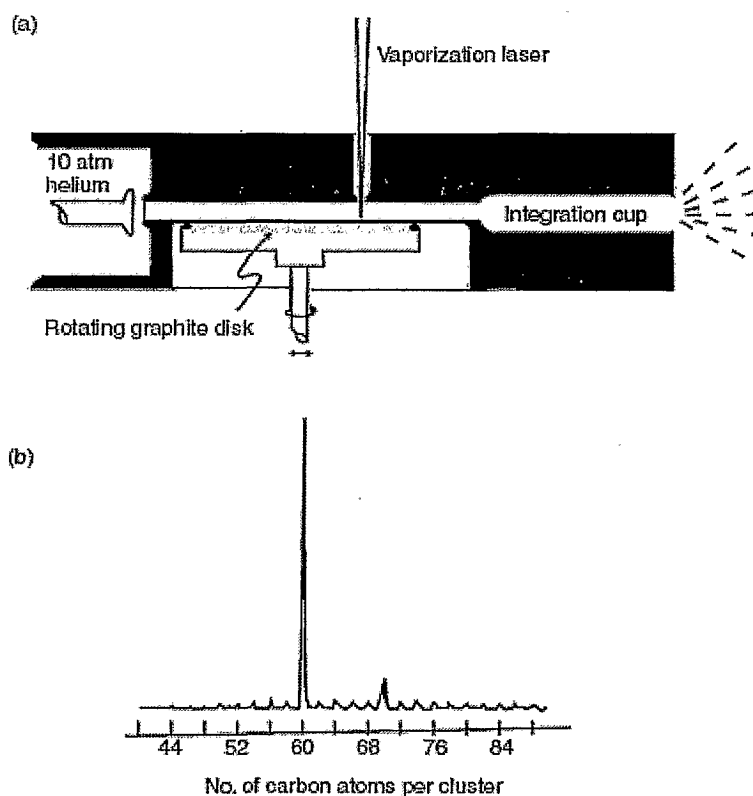


Figure 1.4: hexagonal graphite ((a) Schematic of the pulsed supersonic nozzle used to generate carbon cluster beams. (b) Time-of-flight mass spectra of carbon clusters prepared by laser vaporization of graphite. (From H.W. Kroto, J.R. Heath, S.C. O'Brien, R.F. Curl, and R.E. Smalley. C-60-Buckminsterfullerene, Nature, 318, 162163, 1985.)

with the carbon plasma, confirming the formation of polyynes. They observed two mysterious peaks at mass 720 and, to a lesser extent, 840, corresponding to 60 and 70 carbon atoms, respectively (Fig.1.4b). Further reactivity experiments determined a most likely spherical structure, leading to the conclusion that C_{60} is made of 12 pentagons and 20 hexagons arranged to form a truncated icosahedron[7, 8] (Fig.1.5).

In 1990, at a carbon-carbon composites workshop, Rick Smalley proposed the existence of a tubular fullerene[9]. He envisioned a bucky tube that could be made by elongating a C_{60} molecule. In August of 1991, Dresselhaus followed up in an oral presentation in Philadelphia at a fullerene workshop on the symmetry proposed for

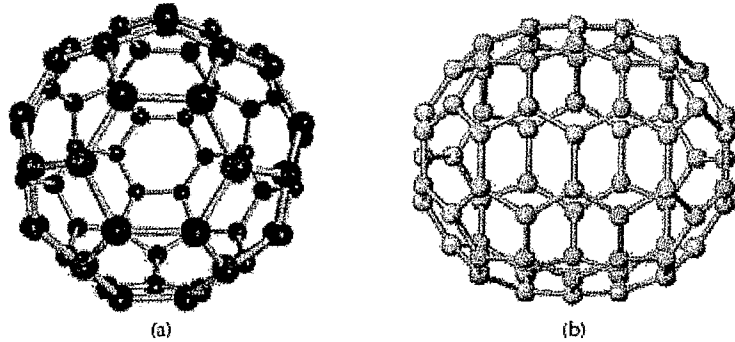


Figure 1.5: Models of the first fullerenes discovered, C_{60} and C_{70} .

carbon nanotubes capped at either end by fullerene hemispheres[10]. Experimental evidence of the existence of carbon nanotubes came in 1991 when Iijima imaged multi-walled carbon nanotubes (MWNTs) using a transmission electron microscope⁶ (Fig.1.6). Two years after his first observation of MWNTs, Iijima and coworkers[11] and Bethune and coworkers[12] simultaneously and independently observed single walled carbon nanotubes (SWNTs).

Although Iijima is credited with their official discovery, carbon nanotubes were probably already observed thirty years earlier from Bacon at Union Carbide in Parma, OH. Bacon began carbon arc research in 1956 to investigate the properties of carbon fibers. He was studying the melting of graphite under high temperatures and pressures and probably found carbon nanotubes in his samples. In his paper, published in 1960, he presented the observation of carbon nanowhiskers under SEM investigation of his material[13] and he proposed a scroll like-structure. Nanotubes were also produced and imaged directly by Endo in the 1970s via high resolution transmission electron microscopy (HRTEM) when he explored the production of carbon fibers by pyrolysis of benzene and ferrocene at $1000C$ [14]. He observed carbon fibers with a hollow core and a catalytic particle at the end. He later discovered that the particle was iron oxide from sand paper. Iron oxide is now well-known as a catalyst in the modern production of

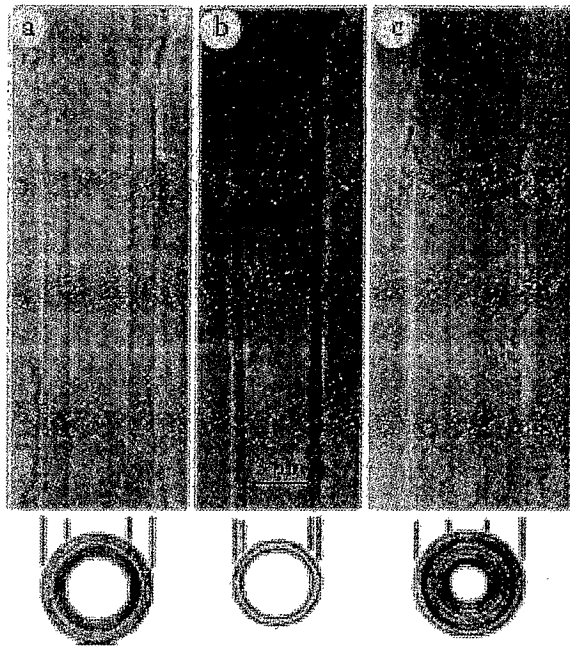


Figure 1.6: Transmission electron micrographs (TEMs) of the first observed multiwalled carbon nanotubes (MWNTs) reported by Iijima in 1991. (From S. Iijima. Helical microtubules of graphitic carbon, *Nature*, 354, 5658, 1991.)

carbon nanotubes.

Although carbon nanotubes were observed four decades ago, it was not until the discovery of C_{60} and theoretical studies of possible other fullerene structures that the scientific community realized their importance. Since this pioneering work, carbon nanotube research has developed into a leading area in nanotechnology expanding at an extremely fast pace.

b)structure

To provide a framework for the presentations in the following chapters, we include in this introductory chapter some definitions about the structure and description of carbon nanotubes.

The structure of carbon nanotubes has been explored early on by high resolution

Transmission Electron Microscopy (TEM) and Scanning Tunneling Microscopy (STM) techniques [15], yielding direct confirmation that the nanotubes are seamless cylinders derived from the honeycomb lattice representing a single atomic layer of crystalline graphite, called a graphene sheet, (Fig.1.7a). The structure of a single-wall carbon nanotube is conveniently explained in terms of its 1D unit cell, defined by the vectors C_h and T in Figure 1.7a.

The circumference of any carbon nanotube is expressed in terms of the chiral vector $C_h = n\hat{a}_1 + m\hat{a}_2$ which connects two crystallographically equivalent sites on a 2D graphene sheet (see Fig.1.7a) [16]. The construction in Figure1.7a depends uniquely on the pair of integers (n,m) which specify the chiral vector. Figure 1.7(a) shows the chiral angle θ between the chiral vector C_h and the "zigzag" direction ($\theta = 0$) and the unit vectors \hat{a}_1 and \hat{a}_2 of the hexagonal honeycomb lattice of the graphene sheet. Three distinct types of nanotube structures can be generated by rolling up the graphene sheet into a cylinder as described below and shown in Figure1.8. The zigzag and armchair nanotubes, respectively, correspond to chiral angles of $\theta = 0$ and 30° , and chiral nanotubes correspond to $0 < \theta < 30^\circ$. The intersection of the vector \overrightarrow{OB} (which is normal to C_h) with the first lattice point determines the fundamental one-dimensional (1D) translation vector T . The unit cell of the 1D lattice is the rectangle defined by the vectors C_h and T [Fig.1.7a].

The cylinder connecting the two hemispherical caps of the carbon nanotube (see Fig.1.8) is formed by superimposing the two ends of the vector C_h and the cylinder joint is made along the two lines \overrightarrow{OB} and $\overrightarrow{AB'}$ in Fig.1.7a. The lines \overrightarrow{OB} and $\overrightarrow{AB'}$ are both perpendicular to the vector C_h at each end of C_h [14]. In the (n,m) notation for $C_h = n\hat{a}_1 + m\hat{a}_2$, the vectors (n, 0) or (0,m) denote zigzag nanotubes and the vectors (n, n) denote armchair nanotubes. All other vectors (n,m) correspond to chiral nanotubes

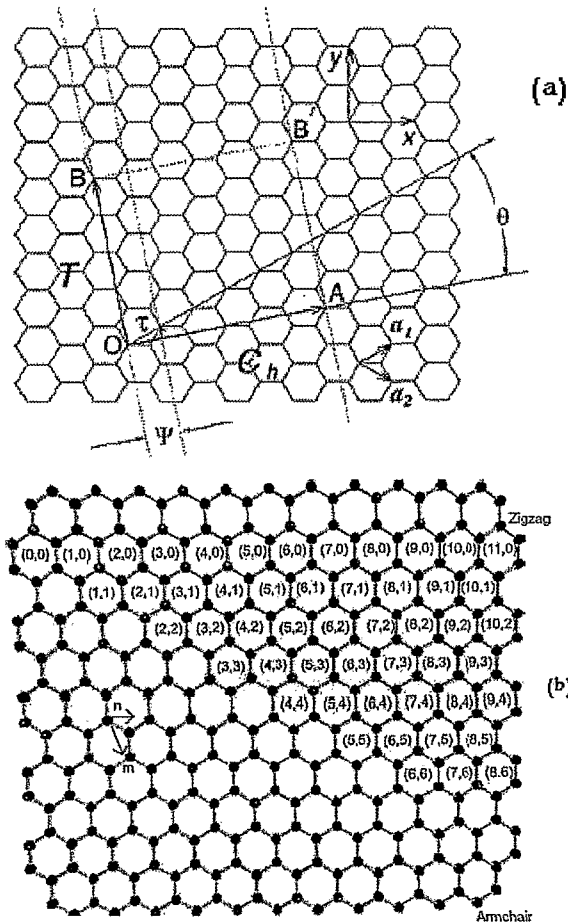


Figure 1.7: (a) The chiral vector \vec{OA} or $C_h = n\hat{a}_1 + m\hat{a}_2$ is defined on the honeycomb lattice of carbon atoms by unit vectors \hat{a}_1 and \hat{a}_2 and the chiral angle θ with respect to the zigzag axis. Along the zigzag axis $\theta = 0^\circ$. Also shown are the lattice vector $\vec{OB} = T$ of the 1D nanotube unit cell and the rotation angle ψ . The diagram is constructed for $(n, m) = (4, 2)$. (b) Possible vectors specified by the pairs of integers (n, m) for general carbon nanotubes, including zigzag, armchair, and chiral nanotubes. Below each pair of integers (n, m) is listed the number of distinct caps that can be joined continuously to the carbon nanotube denoted by (n, m) . The encircled dots denote metallic nanotubes while the small dots are for semiconducting nanotubes